DOI: 10.1021/ma1002112

Macromolecules
ARTICLE

Evaluation of Isoprene Chain Extension from PEO Macromolecular Chain Transfer Agents for the Preparation of Dual, Invertible Block Copolymer Nanoassemblies

Jeremy W. Bartels,[†] Solène I. Cauët,[‡] Peter L. Billings,[†] Lily Yun Lin,[‡] Jiahua Zhu,[§] Christopher Fidge,[‡] Darrin J. Pochan,[§] and Karen L. Wooley*,[‡]

[†]*Department of Chemistry, Washington University in Saint Louis, One Brookings Drive, Saint Louis, Missouri 63130,* [‡]*Department of Chemistry, Department of Chemical Engineering, Texas A&M University, P.O. Box 30012, College Station, Texas 77842-3012, and* [§]*Department of Materials Science and Engineering, Delaware Biotechnology Institute, University of Delaware, Newark, Delaware 19716*

Received January 27, 2010; Revised Manuscript Received July 19, 2010

ABSTRACT: Two RAFT-capable PEO macro-CTAs, 2 and 5 kDa, were prepared and used for the polymerization of isoprene which yielded well-defined block copolymers of varied lengths and compositions. GPC analysis of the PEO macro-CTAs and block copolymers showed remaining unreacted PEO macro-CTA. Mathematical deconvolution of the GPC chromatograms allowed for the estimation of the blocking efficiency, about 50% for the 5 kDa PEO macro-CTA and 64% for the 2 kDa CTA. Self-assembly of the block copolymers in both water and decane was investigated and the resulting regular and inverse assemblies, respectively, were analyzed with DLS, AFM, and TEM to ascertain their dimensions and properties. Assembly of PEO-*b*-PIp block copolymers in aqueous solution resulted in well-defined micelles of varying sizes while the assembly in hydrophobic, organic solvent resulted in the formation of different morphologies including large aggregates and well-defined cylindrical and spherical structures.

Introduction

Interesting chemical, physical, and morphological complexity can be inherited from the self-assembly of amphiphilic block copolymers.[1−7] The generation of micelles in a solvent selective for a portion of the overall block copolymer structure,[8−10] and transformation into their stable, cross-linked variants,[11−13] have been achieved using a wide variety of well-defined multiblock copolymers. Block copolymers within discrete self-assembled particles adopt a range of morphologies and dimensions, giving these micelle-based nanoobjects promise as devices to be applied to the emerging fields of nanomedicine[14−16] and nanomaterials.[17−20]

The properties of polymer assemblies are dependent on the nature of the block copolymer components and their molecular-level organization within the nanoscale framework.[4,5,21] Among the many types of amphiphilic block copolymers that have been investigated,[7,20,22] those containing poly(ethylene oxide) (PEO) as a hydrophilic chain segment, such as PEO-*b*-PCL[16,23,24] and PEO-*b*-PS,[25,26] incorporate a nonionic, antifouling shell layer, which has been shown to be important for biological applications.[27] For instance, PEO-*b*-PCL filomicelle assemblies were capable of *in vivo* blood circulation for several days.[28] In addition to these interesting cylindrical filomicelles, many other morphologies can be accessed from PEO-containing block copolymers.[3,29−32] However, because the PEO segment lacks reactive side chain groups, multifunctionality is often incorporated via the other polymer block segment(s).

The utility of polymer nanostructures, ultimately, relies on access to polymer building blocks that possess well-defined structures and that include functionality. The advent of controlled radical polymerization (CRP)[33−36] has allowed for significantly greater access to functional block copolymer materials[37,38] by a broader scientific population, providing for investigations into increased numbers and types of block copolymer assemblies in the bulk- and solution-states. PEO-*b*-poly(diene) polymers are particularly attractive, because they combine the interesting properties of PEO with reactive, hydrophobic chain segments, which then gives an overall amphiphilic and functional block copolymer structure. Although poly(ethylene oxide)-*block*-polybutadiene[6,39−42] or poly(ethylene oxide)-*block*-polyisoprene, PEO-*b*-PIp,[9,43−45] have long been used for materials applications,[46] their preparation by anionic polymerization methods[47] has hampered their wide-scale availability.

The polymerization of isoprene under controlled radical polymerization conditions has been developed recently, and is emerging as a general method for the preparation of PIp-containing block copolymers (including PEO-*b*-PIp), which is allowing access to functional nanomaterials. Controlled radical polymerization of isoprene was initially reported using nitroxide mediated polymerization (NMP).[9,44,48,49] Diblock copolymers of PEO-*b*-PIp have been successfully prepared by Grubbs and coworkers via NMP methods using a PEO macroinitiator.[9,44] The solution-state properties of nanoassemblies derived from di- and triblock copolymers that include PEO and PIp segments have been investigated, including the formation of micelles and stable vesicles with small molecule additives,[8,21,50] or the formation of unusual assemblies with unique properties when thermoresponsive intermediate blocks were incorporated.[9] Additionally, studies have been performed on PEO-*b*-PIp at various aqueous concentrations, expanding knowledge of the physical properties of the block copolymers as they changed from micelle to gel-like phases.[51]

We were interested in investigating the solution-state assemblies of PEO-*b*-PIp in either water or organic solvents, to afford invertible, functional nanoscale objects, which could carry the reactive PIp units either in the core or the shell. To gain access to

*Corresponding author. E-mail: wooley@mail.chem.tamu.edu.

 Published on Web 08/06/2010 © 2010 American Chemical Society

these block copolymers, reversible addition−fragmentation chain transfer (RAFT) polymerization was employed, because of its tolerance of functional monomers[38,52−59] and our experience with this system.[60−65] Moreover, we were interested in studying in detail the efficiency of RAFT polymerization of isoprene from macromolecular chain transfer agents (macro-CTAs). PEO macro-CTAs were, therefore, generated from simple amidation chemistry of an amino-terminated PEO and an acid-functionalized RAFT agent known to polymerize isoprene readily, and used to afford block copolymers of PEO and PIp that possess interesting physical and solution-state properties.

Previous studies using both dithioester-[66−71] and trithiocarbonate-based[26,29,72,73] PEO macro-CTAs have been reported for the synthesis of well-defined block copolymers with second blocks varying from hydrophilic[67,68,70,71,73] to hydrophobic.[29,66,69,72,74] Problems related to low chain extension efficiency can remain when chain-extending from a hydrophilic polymeric CTA with a hydrophobic monomer, potentially due to the incompatibility between the polymer and the added monomer.[67] The remaining PEO macro-CTA can be removed, typically, using precipitation and/or dialysis techniques, however, this depends upon the chemical nature of the block copolymers obtained and cannot always be achieved. Knowing the exact composition of the final block copolymer and the amount of unreacted macroCTA contaminant is important when preparing nanoassemblies.[1] Incomplete chain extension is readily visible as a low molecular weight component through the use of gel permeation chromatography (GPC), so that mathematical treatment of the chromatograms provides a tool to fully characterize blocking efficiency and final product composition.

Herein, is reported the use of two RAFT-capable, trithiocarbonate-based, PEO macro-CTAs (M_n = 2 and 5 kDa), for the polymerization of isoprene to yield well-defined block copolymers of varied lengths and compositions. Analysis of the GPC chromatograms, including mathematical deconvolution, allowed for estimation of chain extension efficiencies from the PEO macro-CTAs and final product composition. The resultant polymers were investigated for their abilities to assemble in both water and decane, and the resulting regular and inverse micellar nanostructures were analyzed with dynamic light scattering (DLS), atomic force microscopy (AFM), and transmission electron microscopy (TEM).

Experimental Section

Instrumentation. Infrared spectra were obtained on a Perkin−Elmer Spectrum BX FTIR system as neat films on NaCl plates. ^{1}H NMR (300 and 500 MHz) and ^{13}C NMR (75 and 125 MHz) spectra were recorded on either a Varian Mercury 300 MHz or Inova 500 MHz spectrometer using the solvent as internal reference. Glass transition (T_g), melting (T_m), and crystallization (T_c) temperatures were measured by differential scanning calorimetry on a Mettler Toledo DSC822^e (Mettler Toledo Inc., Columbus, OH), with a heating rate of 10 °C/min. Measurements were analyzed using Mettler Toledo Star SW 7.01 software. The T_g was taken as the midpoint of the inflection tangent, upon the third heating scan. Thermogravimetric analysis was performed under N_2 atmosphere using a Mettler Toledo model TGA/SDTA851^e, with a heating rate of 10 °C/min. Measurements were analyzed using Mettler Toledo Star SW 7.01 software. Gel permeation chromatography was conducted on a system equipped with a Waters Chromatography, Inc. (Milford, MA) model 1515 isocratic pump, a model 2414 differential refractometer, and a Precision Detectors, Inc. (Bellingham, MA) model PD-2026 dual-angle (15° and 90°) light scattering detector and a three-column set of Polymer Laboratories, Inc. (Amherst, MA) Styragel columns (PL_{gel} 5 μm Mixed C, 500 Å, and 10^4 Å, 300 × 7.5 mm columns). The system was equilibrated at 35 °C in tetrahydrofuran (THF), which served as the polymer solvent and eluent (flow rate set to 1.00 mL/min). Polymer solutions were prepared at a known concentration (*ca.* 3 mg/mL) and an injection volume of 200 μL was used. Data collection was performed with Precision Detectors, Inc. Precision Acquire software. Data analysis was performed with Precision Detectors, Inc. Discovery 32 software. The differential refractometer was calibrated with standard polystyrene material (SRM 706 NIST), of known refractive index increment dn/dc (0.184 mL/g). The dn/dc values of the analyzed polymers were determined using refractive index detector data. Tapping-mode AFM measurements were conducted in air with a Nanoscope III BioScope system (Digital Instruments, Santa Barbara, CA) operated under ambient conditions with standard silicon tips [type, OTEPSA-70; length (L), 160 lm; normal spring constant, 50 N/m; resonant frequency, 246−282 kHz]. Hydrodynamic diameters (D_h) and distributions for the micelles in aqueous or decane solutions were determined by DLS. The DLS instrumentation consisted of a Brookhaven Instruments Limited (Worcestershire, U.K.) system, including a model BI-200SM goniometer, a model BI-9000AT digital correlator, a model EMI-9865 photomultiplier, and a model 95−2 Ar ion laser (Lexel, Corp., Farmindale, NY) operated at 514.5 nm. Measurements were made at 25 ± 1 °C. Prior to analysis, solutions were filtered through a 0.45 μm Nylon filter (aqueous samples) or not filtered at all (decane). Samples were then centrifuged in a model 5414 microfuge (Brinkman Instruments, Inc., Westbury, NY) for 4 min to remove dust particles. Scattered light was collected at a fixed angle of 90°. The digital correlator was operated with 522 ratio spaced channels and initial delay of 0.5 μs, a final delay of 800 ms, and a duration of 10 min. A photomulitplier aperture of 400 μm was used, and the incident laser intensity was adjusted to obtain a photon counting of 300 kcps. Only measurements in which the measured and calculated baselines of the intensity autocorrelation function agreed to within 0.1% were used to calculate particle size. Particle size distributions were performed with the ISDA software package (Brookhaven Instruments Company), which employed single-exponential fitting, cumulants analysis, and non-negatively constrained least-squares particle size distribution analysis routines. Transmission electron microscopy (TEM) bright-field imaging was conducted on a Hitachi H-7500 microscope, operating at 80 kV. The samples were prepared as follows: 4 μL of a dilute sample solution (with a polymer concentration of ca. 0.2 - 0.5 mg/mL) was deposited onto a carbon-coated copper grid. After 5 min, excess solution was wicked away with a piece of filter paper. The samples were either negatively stained with 4 μL of 1 wt % phosphotungstic acid (PTA) aqueous solution or positively stained with 4 μL of 1% osmium tetroxide aqueous solution. After 1 min, the excess staining solution was wicked away using a piece of filter paper and the samples were left to dry at room temperature overnight prior to imaging.

Materials. Isoprene (Ip) (99%) was obtained from Sigma-Aldrich, Inc. (St. Louis, MO) and was purified by passage over a column of neutral alumina prior to use. Amine-terminated poly(ethylene oxide), 5 kDa and 2 kDa, (Intezyne Laboratories) were used as received. 1-[Dimethylamino)propyl]-3-ethylcarbodiimide methiodide (EDCI) (Aldrich), and hydroxybenzotriazole monohydrate (HOBt) (Novabiochem) were used as received. 1,4-Dioxane (99%), *N*,*N*-dimethylformamide (DMF, 99.8% anhydrous), tetrahydrofuran (THF, 99.9%), dichloromethane (≥99%), diethyl ether, (≥99%, anhydrous), methanol (≥99.9%), di-*tert*-butyl peroxide (98%), were used as received from Sigma-Aldrich. Chloroform-*d* (Cambridge Isotope Laboratories) was used as received. Argon ultrahigh purity grade gas (99.999%) was used as received from Praxair (St. Louis, MO). The RAFT agent, *S*-1-dodecyl-*S*′-(α, α′-dimethyl-α″-acetic acid)trithiocarbonate, **1**, was prepared as previously reported.[75] Because of the high volatility of isoprene and the high temperatures employed in the polymerization thereof, only thick-walled glass flasks, free of visible defects, were used for these experiments, each conducted with at least 50% of the volume of the flask remaining free.[61,62] As further precaution,

all polymerizations were performed in a fume hood with additional shielding. Percent conversions of the isoprene polymerizations were determined using the method of Grubbs and co-workers,[44] where the molecular weight of the isolated polymer was determined with high field ^{1}H NMR spectroscopy (500 MHz) and then set equal to the theoretical molecular weight. While this method does introduce some error (assuming $M_n^{Theory} = M_n^{Actual}$), it is not excessive when compared with the error associated with attempting to determine conversion of isoprene directly.[61]

Synthesis of 5 kDa PEO Macro Chain-Transfer Agent, 2. To a 250 mL round-bottom flask, equipped with a Teflon-coated stirbar, was added chain transfer agent **1** (0.5476 g, 1.579 mmol, 1.5 equiv), EDCI (0.4447 g, 1.497 mmol, 1.5 equiv), and HOBt (0.2037 g, 1.507 mmol, 1.5 equiv). After addition of DMF (50 mL), the flask was sealed with a rubber septum and its contents were allowed to stir for 1 h at ambient temperature. In a separate 250 mL round-bottom flask, monoamino-terminated 5 kDa PEO (5.0023 g, 1.000 mmol, 1.0 equiv, M_n^{GPC} = 7700 Da (polystyrene equivalent)) was dissolved in dichloromethane (30 mL), to which DMF (50 mL) was added. After the contents of the initial round-bottom flask had stirred for 1 h, the 5 kDa PEO solution was added and the reaction mixture was allowed to stir for 4 h at ambient temperature. The product was purified via silica gel-based flash chromatography (eluting with CH_2Cl_2, gradient to 10% MeOH:CH_2Cl_2). The product was dried *in vacuo* overnight, yielding 1.5496 g as a light yellow powder (30% yield). M_n^{NMR} = 7800 Da, M_w^{GPC} = 7900 Da, M_n^{GPC} = 7600 Da (polystyrene equivalent), M_w/M_n = 1.04. T_m = 61.0 °C, T_c = 31.5 °C. T_{decomp} = 395.3 °C. IR (cm^{-1}): 3000−2760, 1672, 1467, 1360, 1343, 1280, 1242, 1148, 1112, 1061, 963, 842, 529. ^{1}H NMR (500 MHz, chloroform-*d*, ppm): δ 3.7−3.5 (br, −C*H*$_2$−C*H*$_2$−O−), 3.5 (s, −O−C*H*$_3$), 3.4 (br, m, −SC(S)S−C*H*$_2$−(CH$_2$)$_{10}$−CH$_3$), 1.9 (s, O−C(O)−C(C*H*$_3$)$_2$−S−), 1.3−1.2 (br, −SC(S)S−CH$_2$−(C*H*$_2$)$_{10}$−CH$_3$), 0.9 (br t, −SC(S)S−CH$_2$−(CH$_2$)$_{10}$−C*H*$_3$). ^{13}C NMR (75 MHz, chloroform-*d*, ppm): δ 173.1, 70.8, 65.3, 58.3, 56.2, 37.1, 32.1, 29.8, 25.6, 22.9, 14.4.

Synthesis of 2 kDa PEO Macro Chain-Transfer Agent, 3. The 2 kDa PEO macro chain-transfer agent, **3**, was prepared following the same procedure as for 5 kDa PEO macro chain-transfer agent, **2**, using chain transfer agent **1** (1.3699 g, 3.757 mmol, 1.5 equiv), EDCI (1.1166 g, 3.759 mmol, 1.5 equiv), HOBt (0.5075 g, 3.756 mmol, 1.5 equiv), monoamino-terminated 2 kDa PEO (5.0019 g, 2.500 mmol, 1.0 eq, M_n^{GPC} = 2500 Da (polystyrene equivalent)), DMF (100 mL) and dichloromethane (30 mL). The reaction yielded 2.7791 g of **3** as a yellowish-white powder (47% yield). ^{1}H NMR spectroscopy confirmed complete functionalization. M_n^{NMR} = 2400 Da, M_w^{GPC} = 3270 Da, M_n^{GPC} = 3200 Da (polystyrene equivalent), M_w/M_n = 1.03. T_m = 50.4 °C, T_c = 9.9 °C. T_{decomp} = 377.5 °C. IR (cm^{-1}): 2990−2770, 1671, 1467, 1360, 1344, 1280, 1242, 1148, 1114, 1061, 946, 843, 530. ^{1}H NMR (500 MHz, chloroform-*d*, ppm): δ 3.6−3.3 (br, −C*H*$_2$−C*H*$_2$−O−), 3.4 (s, −O−C*H*$_3$), 3.2 (br, m, −SC(S)S−C*H*$_2$−(CH$_2$)$_{10}$−CH$_3$), 1.6 (s, O−C(O)−C(C*H*$_3$)$_2$−S−), 1.3−1.2 (br, −SC(S)S−CH$_2$−(C*H*$_2$)$_{10}$−CH$_3$), 0.8 (br t, −SC(S)S−CH$_2$−(CH$_2$)$_{10}$−C*H*$_3$). ^{13}C NMR (75 MHz, chloroform-*d*, ppm): δ 172.6, 70.8, 59.3, 57.3, 40.1, 37.2, 32.1, 29.9, 26.1, 22.9, 14.4.

General Procedure for Synthesis of PEO$_{112}$-*b*-PIp$_{187}$ (4). To a 50 mL bomb-type Schlenk flask equipped with a Teflon coated magnetic stir bar was added Ip (2.5396 g, 37.28 mmol, 373.0 equiv), macro chain transfer agent **2**, (0.5002 g, 0.100 mmol, 1.0 equiv), and di-*tert*-butyl peroxide (0.0070 g, 4.8 × 10^{-5} mol, 0.4 equiv), along with 1,4-dioxane (15 mL). The mixture was degassed via three freeze−pump−thaw cycles. Upon the final thaw the Schlenk flask was backfilled with Ar and placed in a temperature-regulated mineral oil bath set at 125 °C and left to react for 24 h. After cooling the residual solvent and monomer were removed *in vacuo*. Leftover contents of the flask were dissolved in a minimal amount of dichloromethane and precipitated 3 times into 500 mL methanol producing a transparent yellow oil. The excess solvent was decanted off and the product was dried *in vacuo*, yielding 1.035 g (87% yield based on 27% conversion) of sticky yellow powder. M_n^{NMR} = 18 000 Da, M_w^{GPC} = 23 200 Da, M_n^{GPC} = 18 000 Da (polystyrene equivalent), M_w/M_n = 1.28. $(T_g)_{PIp}$ = −60.0 °C, $(T_m)_{PEO}$ = 56.0 °C, $(T_c)_{PEO}$ = 31.4 °C. T_{decomp}: = 401.8 °C. IR (cm^{-1}): 3020−2760, 1726, 1665, 1644, 1466, 1449, 1343, 1280, 1242, 1148, 1114, 1061, 964, 842, 530. ^{1}H NMR (500 MHz, chloroform-*d*, ppm): δ 5.8−5.7 (br, 1,2 C*H*=CH$_2$), 5.2−5.1 (br, 1,4 −CH$_2$−C(CH$_3$)−C*H*−CH$_2$−), 5.0−4.8 (br, 1,2 CH=C*H*$_2$), 4.8−4.6 (br, 4,3 C(CH$_3$)−C*H*$_2$), 3.7−3.5 (br, −C*H*$_2$−C*H*$_2$−O−), 3.4 (s, −O−C*H*$_3$), 3.2 (br, m, −SC(S)S−C*H*$_2$−(CH$_2$)$_{10}$−CH$_3$), 2.2−1.8 (br, C*H*$_2$ isoprene backbone), 1.7−1.5 (br, isoprene backbone C*H*$_3$), 1.6 (s, O−C(O)−C(C*H*$_3$)$_2$−S-), 1.4−1.2 (br, −SC(S)S−CH$_2$−(C*H*$_2$)$_{10}$-CH$_3$), 0.9 (br t, −SC(S)S−CH$_2$−(CH$_2$)$_{10}$−C*H*$_3$). ^{13}C NMR (75 MHz, chloroform-*d*, ppm): δ 147.8, 135.1, 125.2, 124.5, 111.5, 72.2, 70.8, 69.3, 63.7, 62.2, 59.3, 52.2, 44.8, 40.0, 38.7, 32.2, 31.0, 28.5, 26.9, 23.7, 19.0, 16.3, 14.4.

General Procedure for Synthesis of PEO$_{112}$-*b*-PIp$_{47}$ (5). PEO$_{112}$-*b*-PIp$_{47}$, **5**, was prepared following the same procedure as for polymer **4** using the following amounts Ip (1.1927 g, 17.50 mmol, 186.5 equiv), macro transfer agent **2** (0.5016 g, 9.381 × 10^{-5} mol, 1.0 equiv), and di-*tert*-butyl peroxide (0.0041 g, 2.8 × 10^{-5} mol, 0.3 equiv), along with 1,4-dioxane (ca. 5 mL). Purification was attempted repeatedly using precipitation in a variety of hydrophobic and hydrophilic solvents with no success, however a mixture of 400 mL deionized water and 350 mL methanol worked well, yielding a yellow oil. Solvent was removed via rotary evaporation and the remaining polymer was dried *in vacuo*. The final product consisted of 0.4500 g of sticky pale yellow powder (56% yield based on 25% conversion). M_n^{NMR} = 8500 Da, M_w^{GPC} = 11 500 Da, M_n^{GPC} = 8600 Da (polystyrene equivalent), M_w/M_n = 1.34. $(T_g)_{PIp}$ = −61.0 °C, $(T_m)_{PEO}$ = 55.3 °C, $(T_c)_{PEO}$ = 23.0 °C. T_{decomp} = 399.2 °C. IR (cm^{-1}): 2990−2770, 1649, 1466, 1360, 1343, 1280, 1148, 1114, 1061, 946, 842, 668, 530. ^{1}H NMR (500 MHz, dichloromethane-d_2, ppm): δ 5.9−5.8 (br, 1,2 C*H*=CH$_2$), 5.3−5.1 (br, 1,4 −CH$_2$−C(CH$_3$)−C*H*-CH$_2$−), 5.1−4.9 (br, 1,2 CH=C*H*$_2$), 4.9−4.7 (br, 4,3 C-(CH$_3$)−C*H*$_2$), 3.9−3.7 (br, −C*H*$_2$−C*H*$_2$−O−), 3.5 (s, −O−C*H*$_3$), 3.2 (br, m, −SC(S)S−C*H*$_2$−(CH$_2$)$_{10}$−CH$_3$), 2.3−2.0 (br, C*H*$_2$ isoprene backbone), 1.8−1.6 (br, isoprene backbone C*H*$_3$), 1.6 (s, O−C(O)−C(C*H*$_3$)$_2$−S−), 1.4−1.2 (br, −SC(S)S−CH$_2$−(C*H*$_2$)$_{10}$−CH$_3$), 1.0 (br t, −SC(S)S−CH$_2$−(CH$_2$)$_{10}$−C*H*$_3$). ^{13}C NMR (75 MHz, dichloromethane-d_2, ppm): δ 148.0, 135.1, 111.6, 70.8, 59.3, 52.1, 44.9, 40.0, 38.8, 37.2, 32.3, 31.1, 29.9, 28.6, 27.0, 26.0, 23.7, 22.9, 22.3, 16.3, 14.4.

General Procedure for Synthesis of PEO$_{44}$-*b*-PIp$_{60}$ (6). PEO$_{44}$-*b*-PIp$_{60}$, **6**, was prepared following the same procedure as for polymer **4** using the following amounts Ip (0.5089 g, 7.471 mmol, 150 equiv), macro transfer agent **3** (0.1158 g, 4.936 × 10^{-5} mol, 1.0 equiv), and di-*tert*-butyl peroxide (0.0027 g, 1.8 × 10^{-5} mol, 0.3 equiv), along with 1,4-dioxane (ca. 5 mL). The crude product was dissolved in THF and precipitated into ice cold diethyl ether, which yielded a cloudy precipitate. The final product consisted of 0.1990 g of sticky yellow powder (97% yield based on 18% conversion). M_n^{NMR} = 6400 Da, M_w^{GPC} = 8300 Da, M_n^{GPC} = 6500 Da (polystyrene equivalent), M_w/M_n = 1.29. $(T_g)_{PIp}$ = −62.7 °C, $(T_m)_{PEO}$ = 47.3 °C, $(T_c)_{PEO}$ = 12.7 °C. T_{decomp}: = 397.0 °C. IR (cm^{-1}): 3040−2720, 1732, 1660, 1644, 1520, 1466, 1360, 1344, 1280, 1242, 1147, 1114, 1061, 964, 843, 734, 646, 532. ^{1}H NMR (500 MHz, chloroform-*d*, ppm): δ 5.8−5.7 (br, 1,2 C*H*=CH$_2$), 5.2−5.0 (br, 1,4 −CH$_2$−C-(CH$_3$)−C*H*−CH$_2$−), 5.0−4.8 (br, 1,2 CH=C*H*$_2$), 4.8−4.6 (br, 4,3 C(CH$_3$)−C*H*$_2$), 3.7−3.5 (br, −C*H*$_2$−C*H*$_2$−O−), 3.4 (s, −O−C*H*$_3$), 3.2 (br, m, −SC(S)S−C*H*$_2$−(CH$_2$)$_{10}$−CH$_3$), 2.2−1.8 (br, C*H*$_2$ isoprene backbone), 1.7−1.5 (br, isoprene backbone C*H*$_3$), 1.6 (s, O−C(O)−C(C*H*$_3$)$_2$−S−), 1.4−1.2 (br, −SC(S)S−CH$_2$−(C*H*$_2$)$_{10}$−CH$_3$), 0.9 (br t, −SC(S)S−CH$_2$−(CH$_2$)$_{10}$−C*H*$_3$). ^{13}C NMR (75 MHz, chloroform-*d*, ppm): δ 148.0, 135.3, 125.3, 124.5, 111.6, 70.8, 59.3, 52.0, 51.0, 44.9, 42.3, 40.0, 38.8, 37.1, 34.5, 32.2, 30.6, 28.6, 27.0, 26.0, 23.7, 23.0, 16.3, 14.4.

General Procedure for Synthesis of PEO$_{44}$-*b*-PIp$_{43}$ (7). PEO$_{44}$-*b*-PIp$_{43}$, **7**, was prepared following the same procedure as for polymer **4** using the following amounts Ip (0.5224 g, 7.660 mmol,

Scheme 1. Preparation of PEO Macro-CTAs 2 and 3

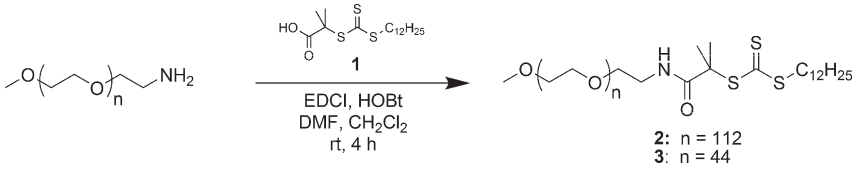

Scheme 2. Preparation of PEO$_n$-*b*-PIp$_m$ Polymers

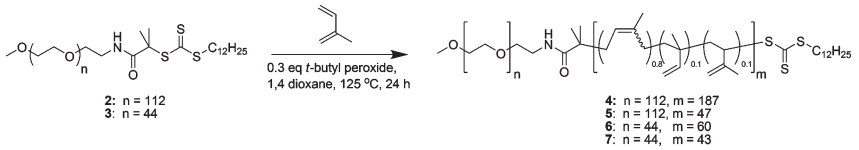

77.0 equiv), macro transfer agent **3** (0.2251 g, 9.595×10^{-5} mol, 1.0 equiv), and di-*tert*-butyl peroxide (0.0050 g, 3.4×10^{-5} mol, 0.3 equiv), along with 1,4-dioxane (ca. 5 mL). The crude product was dissolved in THF and precipitated into ice cold diethyl ether which yielded a cloudy precipitate. The final product consisted of 0.3302 g of sticky yellow powder (88% yield based on 27% conversion). $M_n^{NMR} = 5500$ Da, $M_w^{GPC} = 6900$ Da, $M_n^{GPC} = 5300$ Da (polystyrene equivalent), $M_w/M_n = 1.30$. $(T_g)_{PIp} = -64.5$ °C, $(T_m)_{PEO} = 49.0$ °C, $(T_c)_{PEO} = 42.5$ °C. T_{decomp}: = 399.5 °C. IR (cm^{-1}): 2990−2770, 1733, 1644, 1523, 1466, 1360, 1344, 1280, 1242, 1147, 1112, 1061, 946, 842, 530. ^{1}H NMR (500 MHz, chloroform-*d*, ppm): δ 5.8−5.7 (br, 1,2 C*H*═CH$_2$), 5.2−5.1 (br, 1,4 −CH$_2$−C(CH$_3$)−C*H*−CH$_2$−), 5.0−4.8 (br, 1,2 CH═C*H*$_2$), 4.8−4.6 (br, 4,3 C(CH$_3$)−C*H*$_2$), 3.7−3.5 (br, −C*H*$_2$−C*H*$_2$−O−), 3.4 (s, −O−C*H*$_3$), 3.2 (br, m, −SC(S)S−C*H*$_2$−(CH$_2$)$_{10}$−CH$_3$), 2.2−1.8 (br, C*H*$_2$ isoprene backbone), 1.7−1.5 (br, isoprene backbone C*H*$_3$), 1.6 (s, O−C(O)−C(C*H*$_3$)$_2$−S−), 1.4−1.2 (br, −SC(S)S−CH$_2$−(C*H*$_2$)$_{10}$−CH$_3$), 0.9 (br t, −SC(S)S−CH$_2$−(CH$_2$)$_{10}$−C*H*$_3$). ^{13}C NMR (75 MHz, chloroform-*d*, ppm): δ 178.1, 148.0, 135.3, 129.1, 125.3, 124.5, 111.6, 72.2, 70.8, 67.0, 63.9, 59.3, 52.1, 50.9, 44.9, 42.3, 40.0, 38.8, 37.2, 32.2, 31.1, 29.9, 28.5, 27.0, 26.0, 23.7, 23.0, 18.3, 17.5, 16.3, 14.4.

Preparation of Polymer Micelles 8. In a 100 mL, round-bottom flask equipped with a magnetic stirring bar, diblock copolymer **4** (14.8 mg, 8.22×10^{-6} mol) was dissolved in DMF (15.0 mL), yielding a transparent pale yellow solution. Water (15 mL) was added dropwise via a syringe pump, complete with vigorous stirring, over a period of 3 h, resulting in a clear solution. The mixture was transferred to dialysis tubing (MWCO 3500 Da) and was dialyzed against DI water for 3 days to result in 37 mL of micelle solution. For TEM imaging, phosphotungstic acid was used as a negative stain and osmium tetroxide (OsO4) as a positive stain. Final concentration: 0.58 mg/mL. Hydrodynamic diameter (DLS): $(D_h)_i = 154 \pm 49$ nm, $(D_h)_v = 93 \pm 37$ nm, $(D_h)_n = 54 \pm 38$ nm. D_{av}(TEM) = 55 ± 18 nm. H (AFM) = 8 ± 3 nm.

Preparation of Polymer Micelles 9. The same procedure as performed to produce micelle solution **8** was followed using diblock copolymer **5** (16.3 mg, 1.91×10^{-5} mol), affording micelle solution **9.** Final concentration: 1.95 mg/mL. Hydrodynamic diameter (DLS): $(D_h)_i = 114 \pm 9$ nm, $(D_h)_v = 26 \pm 4$ nm, $(D_h)_n = 18 \pm 4$ nm. D_{av} (TEM) = 31 ± 4 nm. H (AFM) = 4 ± 1 nm.

Preparation of Polymer Micelles 10. The same procedure as performed to produce micelle solution **8** was followed using diblock copolymer **6** (5.0 mg, 7.8×10^{-7} mol), affording micelle solution **10**. Final concentration: 3.17 mg/mL. Hydrodynamic diameter (DLS): $(D_h)_i = 83 \pm 12$ nm, $(D_h)_v = 31 \pm 8$ nm, $(D_h)_n = 21 \pm 6$ nm. D_{av}(TEM) = 30 ± 5 nm. H (AFM) = 4 ± 1 nm.

Preparation of Polymer Micelles 11. The same procedure as performed to produce micelle solution **8** was followed using diblock copolymer **7** (20.0 mg, 3.6×10^{-5} mol), affording micelle solution **11**. Final concentration: 1.4 mg/mL. Hydrodynamic diameter (DLS): $(D_h)_i = 32 \pm 9$ nm, $(D_h)_v = 18 \pm 4$ nm, $(D_h)_n = 15 \pm 4$ nm. D_{av}(TEM) = 18 ± 3 nm. H (AFM) = 2 ± 1 nm.

Preparation of Inverse Polymer Micelles 12. In a 100 mL round-bottom flask equipped with a magnetic stirring bar was dissolved diblock copolymer **4** (13.8 mg, 6.4×10^{-6} mol) in THF (15.0 mL), yielding a transparent pale yellow solution. Decane (25 mL) was added dropwise via a syringe pump, complete with vigorous stirring, over a period of 2 h, resulting in an opaque solution. Final concentration: 0.35 mg/mL. Hydrodynamic diameter (DLS): $(D_h)_i = 569 \pm 142$ nm, $(D_h)_v = 515 \pm 160$ nm, $(D_h)_n = 252 \pm 167$ nm. (cylindrical micelles) D_{av}(TEM) = 34 ± 6 nm, (spherical micelles) D_{av}(TEM) = 25 ± 3 nm. H (AFM) = 11 ± 2 nm.

Preparation of Inverse Polymer Micelles 13. The same procedure was performed to produce micelle solution **12** was followed using diblock copolymer **5** (13.7 mg, 1.61×10^{-5} mol), affording micelle solution **13**. Final concentration: 0.34 mg/mL. Hydrodynamic diameter (DLS): $(D_h)_i = 556 \pm 102$ nm, $(D_h)_v = 641 \pm 134$ nm, $(D_h)_n = 434 \pm 76$ nm. D_{av}(TEM) = 117 ± 42 nm. H (AFM) = 6 ± 1 nm.

Preparation of Inverse Polymer Micelles 14. The same procedure was performed to produce micelle solution **12** was followed using diblock copolymer **6** (5.9 mg, 9.2×10^{-7} mol), affording micelle solution **14**. Final concentration: 0.20 mg/mL. Hydrodynamic diameter (DLS): $(D_h)_i = 414 \pm 122$ nm, $(D_h)_v = 487 \pm 187$ nm, $(D_h)_n = 308 \pm 84$ nm. D_{av}(TEM) = 179 ± 54 nm. H (AFM) = 7 ± 2 nm.

Preparation of Inverse Polymer Micelles 15. The same procedure was performed to produce micelle solution **12** was followed using diblock copolymer **7** (12.7 mg, 2.3×10^{-5} mol), affording micelle solution **15**. Final concentration: 0.32 mg/mL. Hydrodynamic diameter: D_{av}(TEM) = 356 ± 71 nm. H (AFM) = 4 ± 2 nm. DLS did not yield suitable correlation for data analysis.

Results and Discussion

Monofunctional RAFT PEO macro-CTAs **2** and **3** were prepared through amidation reaction between acid-functionalized RAFT agent DDMAT, **1**, and monoamino-functionalized PEO polymers of 5 and 2 kDa molecular weight, respectively (Scheme 1). The macro-CTAs were obtained in modest yield, however moderate losses likely occurred during the chromatography required to purify the final product. The chain ends of the α-methoxy group (at ~3.2 ppm) and the ω-dodecyl group (at ~0.9 ppm) were visible in the ^{1}H NMR spectra and the integration of their respective peaks agreed with a 1:1 theoretical ratio (see Supporting Information). The PEO macro-CTAs, therefore, showed complete trithiocarbonate functionality by ^{1}H NMR spectroscopy, which allowed for polymerization of isoprene for the formation of amphiphilic block copolymers.

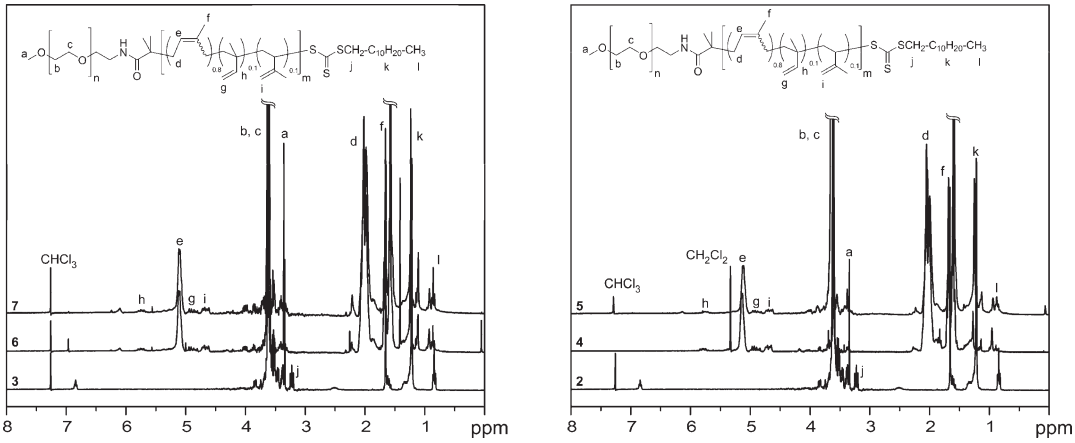

Figure 1. ^{1}H NMR spectra (500 MHz, $CDCl_3$ and CD_2Cl_2) for 5 kDa PEO-block series, macro-CTA **2**, and PEO-*b*-PIp block copolymers **4** and **5** (left), and 2 kDa PEO-block series, macro-CTA **3**, and PEO-*b*-PIp block copolymers **6** and **7** (right).

Table 1. Molecular Weight, Polydispersity, and Thermal Analysis Data for PEO Macro-CTAs and PEO-*b*-PIp Block Copolymers

polymer	M_n^{NMR} (Da)	M_n^{GPC} (Da)[a]	mol % PIp	PDI[a]	T_g (°C)[b]	T_m (°C)[c]	T_{decomp} (°C)
2	7800	7600	n/a	1.04	n/a	61.0	395.3
3	2400	3200	n/a	1.03	n/a	50.4	377.5
4	18 000	18 000	71	1.28	−60.0	56.0	401.8
5	8500	8600	38	1.34	−61.0	55.3	399.2
6	6400	6500	64	1.29	−62.7	47.3	397.0
7	5500	5300	53	1.30	−64.7	49.0	399.5

[a] Predialysis value. [b] Polyisoprene region. [c] Poly(ethylene oxide) region.

Differing degrees of isoprene chain extension from the two macro-CTAs gave a series of block copolymers having variation in the hydrophilic−hydrophobic balance and overall polymer chain lengths, by control of the relative individual block lengths. Two lengths of poly(isoprene) were chain extended from each PEO precursor, **2** and **3** (Scheme 2), using standard RAFT conditions. The initial reaction mixtures of **2** or **3** in 1,4-dioxane, to which is added isoprene and then *tert*-butyl peroxide, existed as opaque heterogeneous poorly dissolved solutions. After only ca. 1 h of heating at 125 °C, as the polymerization progressed, the solutions became transparent, and had reached ca. 25−30% conversion of isoprene after 24 h. The polymers were obtained in high yields by precipitation into methanol for polymer **4**, methanol/water for polymer **5** and cold diethyl ether for polymers **6** and **7**. For polymer **5**, the high weight fraction of PEO rendered methanol inadequate as a nonsolvent for the block and water had to be added to allow for the precipitation to occur. All precipitated polymers were dried *in vacuo* to remove remaining traces of monomer and solvent. Polymers **4**-**7** had interesting solubility properties across a wide range of solvent polarity showing a potential ability to spontaneously form assemblies in different solvents. This finding triggered our consideration of the invertible nature that the assemblies might possess in both aqueous conditions and in a hydrophobic environment such as decane.[22,76]

Both ^{1}H and ^{13}C NMR spectroscopy were used to determine the compositions of the polymers (Figure 1, ^{13}C NMR spectra available in Supporting Information) and to confirm the removal of nonreacted isoprene monomer. The final degree of polymerization of isoprene was determined using ^{1}H NMR by integration of the vinyl peaks of the polyisoprene block against the methoxy peak of the PEO chain end. In addition, thermogravimetric analysis (TGA) and differential scanning calorimetry (DSC) were performed to assess thermal properties for the block copolymers. Results are presented with molecular weight and polydispersity data in Table 1 (TGA/DSC figures available in Supporting Information). Longer block lengths of both PEO and PIp resulted in higher glass transition temperatures. As would be expected, incorporation of isoprene resulted in lower melting transition temperatures of the PEO block.

In order to better understand the relationship between polymer size/composition and structure obtained during solution assembly, accurate determination of block sizes must be obtained. GPC analysis of the PEO macro-CTAs and block copolymers (Figure 2) showed that unreacted PEO macro-CTA remained present in all block copolymer samples. The apparent agreement between molecular weights calculated by NMR and GPC is believed to be an artifact of polymer composition, structure and of the GPC measurement itself for these particular samples. Multipeak mathematical deconvolution of the peaks (Figure 4) enabled the calculation of M_n for both the block copolymer and remaining PEO macro-CTA with respect to the polystyrene calibration curve (Table 2). The elution volume of the low molecular weight shoulder present in the chromatogram of the block copolymers corresponded to that of the PEO macro-CTA and the molecular weight calculated for the shoulder corresponded to that obtained for the PEO macro-CTA itself. It is unlikely that this remaining PEO macro-CTA is nonfunctional as thorough ^{1}H NMR analysis of the PEO macro-CTAs after column chromatography showed good correlation between methoxy chain-end and dodecyl chain-end of the trithiocarbonate demonstrating high functionality of the macro-CTAs (see Supporting Information). A variety of factors can cause incomplete chain extension or blocking including low functionality of the chain-transfer agent or low chain-extension efficiency. It is believed that incompatibility between the hydrophilic macro-CTA and hydrophobic isoprene monomer could be a major contributor to low or slow chain-transfer in this case.

In order to confirm the nature of the low molecular weight shoulder, a fraction was collected between 23 and 25 min of the GPC run of polymer **6**, Figure 2. Analysis of the fraction by ^{1}H NMR spectroscopy showed peaks corresponding to the α-methoxy and ω-dodecyl chain ends of the PEO macro-CTA and their integration gave a 1:1 ratio, Figure 3. The degree of polymerization

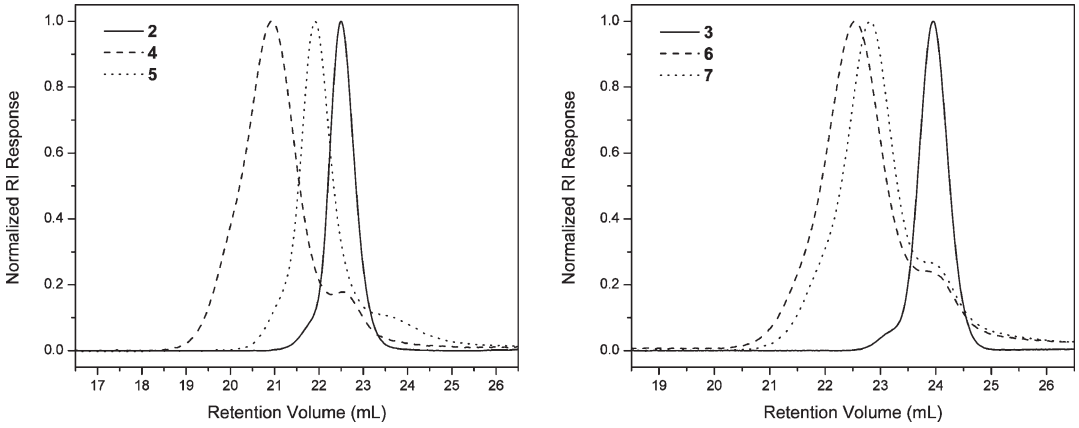

Figure 2. THF−GPC chromatograms of 5 kDa PEO-block series, macro-CTA **2**, and PEO-*b*-PIp block copolymers **4** and **5** (left) and 2 kDa PEO-block series, macro-CTA **3**, and PEO-*b*-PIp block copolymers **6** and **7** (right).

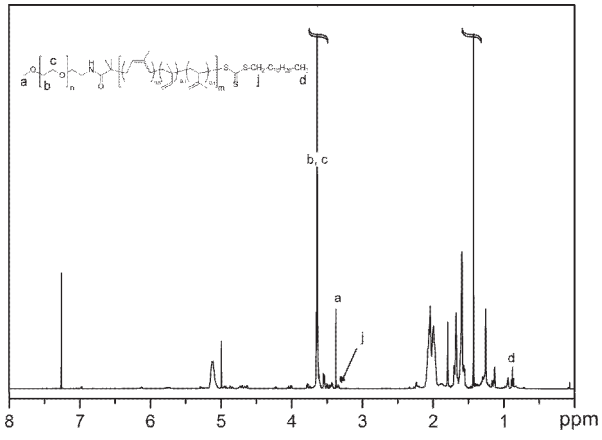

Figure 3. ^{1}H NMR spectrum (500 MHz, $CDCl_3$) for 23 to 25 min fraction of the GPC run of PEO-*b*-PIp block copolymer **6**.

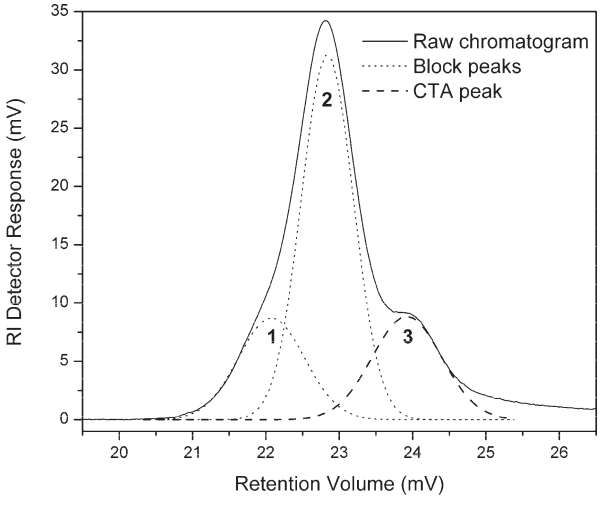

Figure 4. Example of multipeak mathematical deconvolution of GPC chromatogram of polymer **7**. A_{block} corresponds to the area of peaks 1 + 2 and A_{CTA} corresponds to the area of peak 3.

of the PEO calculated from the integration of the PEO methylene peaks against both CTA chain ends corresponded to that of the macro-CTA. This seemed to indicate the presence of unreacted PEO macro-CTA. However, from the comparison of Figures 1 and 3, it also appears that peak j, S−CH_2, clearly present in the spectra of the PEO macro-CTAs is not as pronounced in the spectra of the block copolymers or the extracted fraction. This reduction in signal

Table 2. M_n Values for Low and High Molecular Weight Peaks, d*n*/d*c* of Block Copolymers and Blocking Efficiency Calculated from Multi-Peak Mathematical Deconvolution of GPC Chromatograms and Other GPC Data

polymer	$M_{n,shoulder}^{GPC}$ (Da)	$M_{n,block}^{GPC}$ (Da)	d*n*/d*c*	blocking efficiency
4	7700	22 900	0.1076	0.46
5	4200	11 800	0.0911	
6	3100	8300	0.1057	0.63
7	3000	7000	0.1029	0.65

intensity could be an indicator of the incorporation of isoprene monomer units on the CTA resulting in a shift and broadening of peak j. Addition of a few units of isoprene to the CTA would also explain the difficulty of purification of the block copolymers even in a good solvent for PEO homopolymer. The lack of further extension of the isoprene block could be due to configurations and/or conformations unfavorable to further monomer attachment. The low molecular weight shoulder, therefore, appeared to be either unreacted PEO or PEO with very few isoprene monomer units added, each retaining the trithiocarbonate chain transfer unit, or a mixture of both.

Because of the presence of unreacted PEO macro-CTA, the DP of isoprene as calculated by ^{1}H NMR spectroscopy is inexact. In order to calculate the actual DP of isoprene the unreacted PEO macro-CTA should be removed. Dialysis was performed on each of the copolymers against water for 5 days to attempt to remove unreacted starting material, with mixed results. Therefore, an estimation of the amount of unreacted PEO macro-CTA present and blocking efficiency was carried out through mathematical deconvolution of GPC chromatograms.

Following the method used by Gao et al.,[77] gel permeation chromatography was used to estimate the chain extension efficiency of the PEO macro-CTAs for each polymerization. Mathematical deconvolution of the GPC chromatograms provided a multipeak fitting for all polymer peaks with a low molecular weight peak corresponding to the "unreacted" macro-CTA and one or several peaks corresponding to the actual block copolymer, Figure 4. According to the study on the homopolymerization of isoprene by Germack and Wooley,[61] the conditions, which were similar to those included in this work, did not yield uncontrolled, thermally promoted self-polymerization of isoprene and did not result in any significant chain−chain coupling. Peak 1 of Figure 4 is, therefore, expected to be due in part to the higher molecular weight component visible in the PEO-CTAs undergoing chain extension. Some chain−chain coupling or branching along the polyisoprene backbone can also account for the high molecular

weight component. Although ^{1}H NMR integrations showed no components other than PEO and PEO-*b*-PIp, unfortunately, there was an unassignable low molecular weight component in **5**, which prevented it from being able to be analyzed according to this deconvolution routine. Using the polystyrene calibration of the DRI detector it was possible to calculate M_n for each component individually, M_{CTA} the molecular weight of the remaining PEO macro-CTA, peak 3, and M_{block} the molecular weight of the block copolymer, peaks 1 and 2. Although the ratio of apparent to real molecular weight varies from PEO to PIp homopolymers the difference of separation is small and we, therefore, decided to use M_n from GPC as an estimation of molecular weight in the following calculations. Values of dn/dc for PEO macro-CTAs and for pure polyisoprene were determined as 0.0740 and 0.1246 respectively using response vs concentration plots from the differential refractometer. Values of dn/dc for the "pure" block copolymers were calculated following eq 1 using the calculated M_n of the peaks (Table 2) and the (dn/dc) values for PEO macro-CTAs and pure polyisoprene determined earlier.

$$\left(\frac{dn}{dc}\right)_{block} = w_{CTA} \times \left(\frac{dn}{dc}\right)_{CTA} + w_{IP} \times \left(\frac{dn}{dc}\right)_{IP} \quad (1)^{78}$$

with w_{CTA} and w_{IP} weight fractions of PEO-CTA and polyisoprene in block copolymer sample, calculated using M_n of the CTA peak and block copolymer peak (Table 2).

The instantaneous response from the DRI detector at a given retention volume i, R_i, is given by eq 2. The area of a peak on the GPC chromatogram, A_P, can be expressed as a sum of the response from the DRI detector over the elution volume of the peak, eq 3.

$$R_i = k \times \left(\frac{dn}{dc}\right)_i \times c_i \quad (2)$$

Scheme 3. Schematic Illustrations of the Aqueous Assembly of 4−7 To Give Micelles 8-11, Respectively, and Decane Assembly of 4−7 To Give Inverse Micellar Assemblies 12−15, Respectively

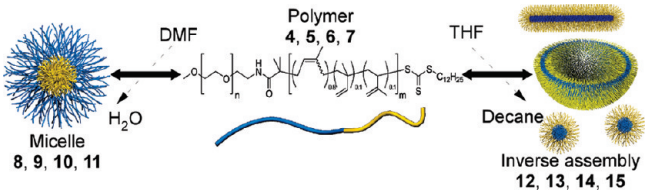

with k DRI detector constant, $(dn/dc)_i$ specific refractive index of the fraction (mL/g) and c_i instantaneous mass concentration in retention volume i (g/mL).

$$A_P = \sum_{i=0}^{N} R_i \times \Delta V = \sum_{i=0}^{N} k \times \left(\frac{dn}{dc}\right)_i \times c_i \times \Delta V$$

$$A_P = k \sum_{i=0}^{N} \left(\frac{dn}{dc}\right)_i \times m_i \quad (3)$$

with $m_i = c_i \times \Delta V$ instantaneous mass of polymer in retention volume i and ΔV volume fraction measured.

Equation 3 can be simplified to express A_P as a function of dn/dc of the polymer, M_n of the polymer and number of moles of polymer in the sample. The area of the peak corresponding to the unreacted macro-CTA, A_{CTA}, and the total area of the peak corresponding to the block copolymer, A_{block}, have been expressed in this way in eqs 4 and 5, respectively.

$$A_{CTA} = k\left(\frac{dn}{dc}\right)_{CTA} \times M_{CTA} \times n_{CTA} \quad (4)$$

with n_{CTA} being the number of moles of remaining macro-CTA.

$$A_{block} = k\left(\frac{dn}{dc}\right)_{block} \times M_{block} \times n_{block} \quad (5)$$

with n_{block} number of moles of block copolymer in the sample.

$$x_b = \frac{\frac{A_{block}}{A_{CTA}} \times \left(\frac{dn}{dc}\right)_{CTA} \times M_{CTA}}{\left(\frac{dn}{dc}\right)_{block} \times M_{block} + \frac{A_{block}}{A_{CTA}} \times \left(\frac{dn}{dc}\right)_{CTA} \times M_{CTA}} \quad (6)$$

Finally, the mole fraction of block copolymer or blocking efficiency, x_b, can be developed from eq 4 and 5 to get eq 6 in which all terms have either been previously calculated or measured from the GPC chromatogram. Using eq 6, it was possible to calculate the blocking efficiency for polymers **4**, **6** and **7** (Table 2). The blocking efficiency was estimated to be around 46% for the 5 kDa and 64% for the 2 kDa PEO macro-CTA polymer series. The length of the PEO macro-CTA seems to have an influence on the blocking efficiency for the chain extension of isoprene, however, the effect of the PEO macro-CTA chain length on the extension of other hydrophobic monomers has not yet been reported. In

Table 3. Micellization Data (Aqueous Solution)

micelle	D_h(Int.), nm	D_h(Vol.), nm	D_h(Num.), nm	D(TEM)[a], nm	D_{core}(TEM),[b,c] nm	height (AFM), nm
8	154 ± 49	93 ± 37	54 ± 38	55 ± 18	30 ± 6	8 ± 3
9	114 ± 9	26 ± 4	18 ± 4	31 ± 4	13 ± 3	4 ± 1
10	83 ± 12	31 ± 8	21 ± 6	30 ± 5	24 ± 5	4 ± 1
11	32 ± 9	18 ± 4	15 ± 4	18 ± 3	8 ± 2	2 ± 1

[a] Phosphotungstic acid stain. [b] OsO_4 stain. [c] See Figure S9, Supporting Information for images.

Table 4. Inverse Micellization Data (Decane Solution)

micelle	D_h(Int.), nm	D_h(Vol.), nm	D_h(Num.), nm	D(TEM)[a], nm	height (AFM), nm
12	569 ± 142	515 ± 160	252 ± 167	34 ± 6[c] 25 ± 3[d]	11 ± 2
13	556 ± 102	641 ± 134	434 ± 76	e	6 ± 1
14	414 ± 122	487 ± 187	308 ± 84	e	7 ± 2
15	b	b	b	e	4 ± 2

[a] OsO_4 stain. [b] Insufficient correlation. [c] cylindrical inverse micelle. [d] spherical inverse micelle. [e] the dimensions of the assemblies could not be accurately determined, as they are not confirmed as spherical or vesicular in nature.

order to obtain more accurate blocking efficiency values, this method should be used for polymers of similar chemical compositions where the components have similar K and α values.

Block copolymers **4**−**7**, respectively, were assembled into micelles using solvent-induced micellization procedures, giving water-stable micelles **8**−**11** and decane-stable inverse assemblies **12**−**15** (Scheme 3). Our interest in the dual assembly of these materials was several-fold: (1) the interesting solution-state properties for the block copolymer during attempts at precipitation for purification of the materials; (2) the antifouling characteristics of PEO, the reactivity and cross-linkability of PIp, and the ability to partition those distinctly different materials into different domains; (3) the effects also that might result from having residual homopolymer[79] present in the form of nonchain extended PEO-macroCTA. The resulting structures were analyzed via DLS, AFM, and TEM to evaluate the type of morphologies obtained and their domain sizes (Tables 3 and 4).

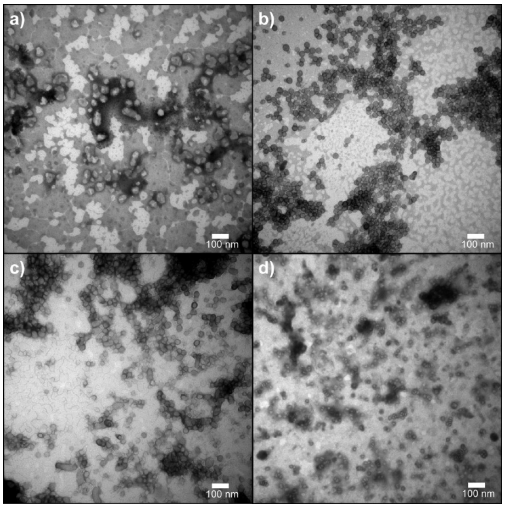

Figure 5. TEM images of PEO-*b*-PIp diblock copolymer aqueous micelles **8**, **9**, **10**, and **11** using phosphotungstic acid as negative stain.

Aqueous-based micellization was achieved through the dissolution of block copolymers **4**−**7** into DMF followed by the slow addition of an excess of water. The micellar solutions, **8**−**11**, were then dialyzed against nanopure water for several days to remove traces of organic solvent. All of the block copolymers readily formed monomodal aqueous spherical micelles, whose particle diameters followed trends relative to the parent copolymer, *e.g.*, longer block length PEO relative to PIp gave smaller particles, and shorter overall polymer chain length afforded smaller particle assemblies. These trends, summarized in Table 3, can be easily observed through DLS data, located in Supporting Information, and on both negatively and positively stained TEM images (Figures 5 and S9, respectively).

As measured by TEM, block copolymer **4** formed large particles of 55 ± 18 nm diameter with slight irregularities, whereas **5** formed more regularly shaped particles of 31 ± 4 nm diameter, with the smaller deviation reflecting the particle quality. The particles were also analyzed by AFM to obtain an estimate of particle height on a mica substrate (Figure 6). Although the TEM and DLS diameter values were in good agreement, the AFM-measured heights were substantially low, which is likely due to an affinity of the PEO shell for the hydrophilic mica surface, perhaps combined with PEO crystallization events that occur upon drying,

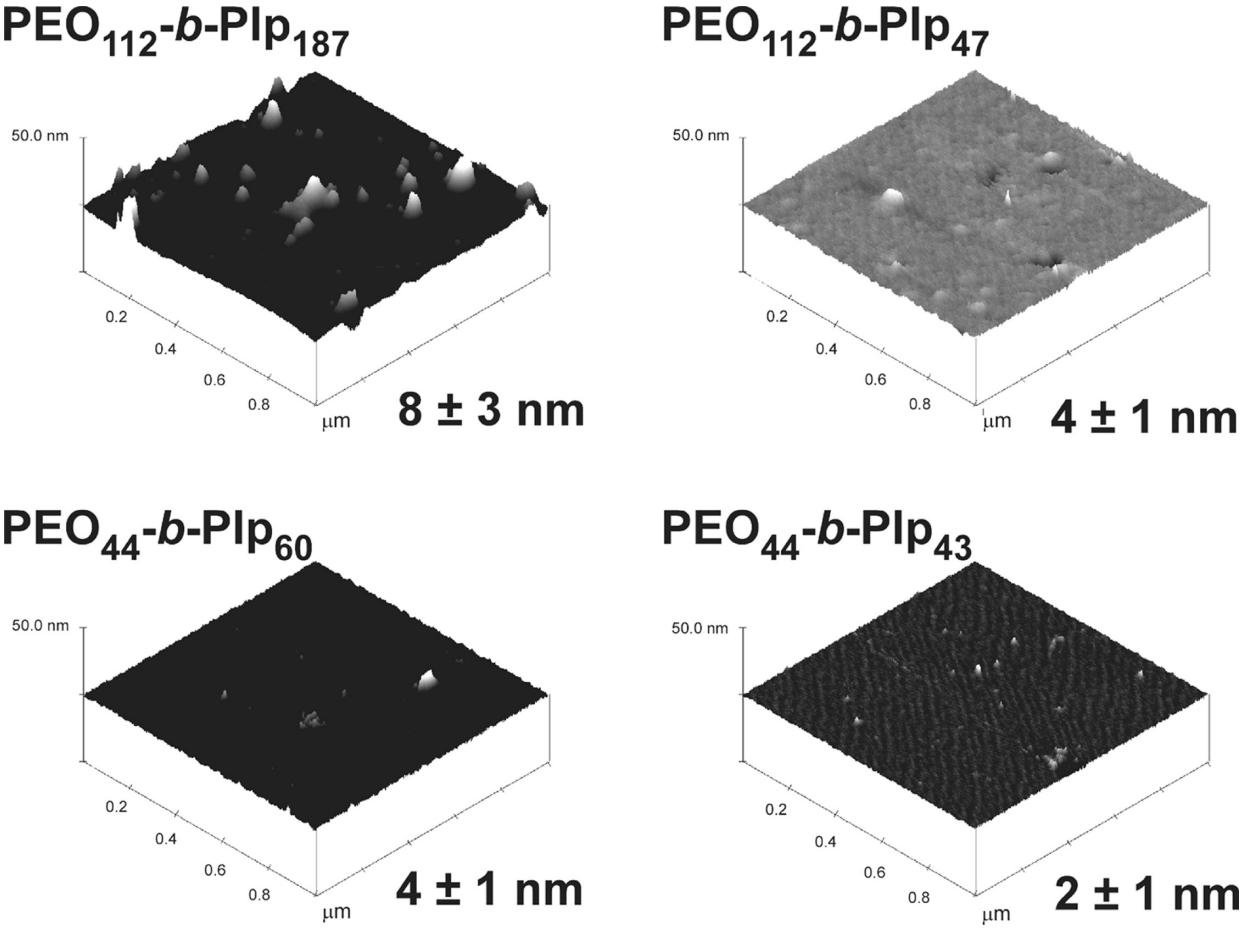

Figure 6. AFM images PEO-*b*-PIp diblock copolymer aqueous micelles **8**, **9**, **10**, and **11**, together with average height values.

resulting in a spreading and reorganization of micelle structure as has been noted before for this block copolymer system by Glynos et al.[45] The combination of these data demonstrates that the PEO-*b*-PIp block copolymers can readily form well-defined micelles of varying sizes in aqueous solution.

To determine how the polymers assemble in hydrophobic solvent, micellization conditions were altered to induce formation of inverse micelles in decane. Decane provides a hydrophobic nonreactive solvent environment with a high boiling point. Inverse assemblies, **12**−**15**, of block copolymers **4**−**7**, respectively, were obtained through dissolution the copolymers into THF followed by the slow addition of an excess of decane. It should be noted that post-assembly dialysis was not performed, as had been done for the aqueous micelles, due to solvent cost. All solutions had minute amounts of precipitate that appeared postassembly.

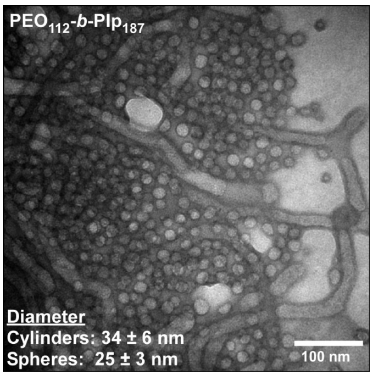

Figure 7. TEM images of PEO-*b*-PIp diblock copolymer inverse assemblies **12** using OsO_4 as positive stain.

Each block copolymer readily formed assemblies of interesting sizes and morphologies, yet each was heterogeneous. DLS analysis of the assemblies **12**−**14** showed larger structures, in comparison to the aqueous assemblies (see Supporting Information for representative DLS figures or Table 4 for listing). In the case of assembly **12**, sub-100 nm structures were also present. DLS examination of inverse micelle **15** yielded insufficient correlation, and further attempts to inspect the solution post-centrifugation and filtration yielded no results. TEM analysis of assembly **12**, stained using OsO_4-stain, which selectively stains PIp, showed bundled mixtures of long cylinders and sub-100 nm spheres (Table 4) which was also confirmed by DLS and AFM (Figures 7 and 8). AFM and DLS analysis of assemblies **13**−**15** showed larger aggregates (Figure 8 and Table 4), consistent with vesicles, but the exact nature of these supramolecular structures could not be confirmed by TEM. Because of the difficulties in performing cryo-TEM with high boiling and crystallizable solvents, such as decane, attempts to obtain cryo-TEM images were unsuccessful. The assembly of PEO-*b*-PIp block copolymers in hydrophobic, organic solvent resulted in the formation of either a mixture of cylindrical and spherical morphologies or large aggregates of sizes consistent with vesicular structures, depending on the block lengths.

Conclusions

Highly interesting, multifunctional, amphiphilic PEO-*b*-PIp block copolymers were prepared via RAFT polymerization, for which challenges were encountered, yet well-defined structures

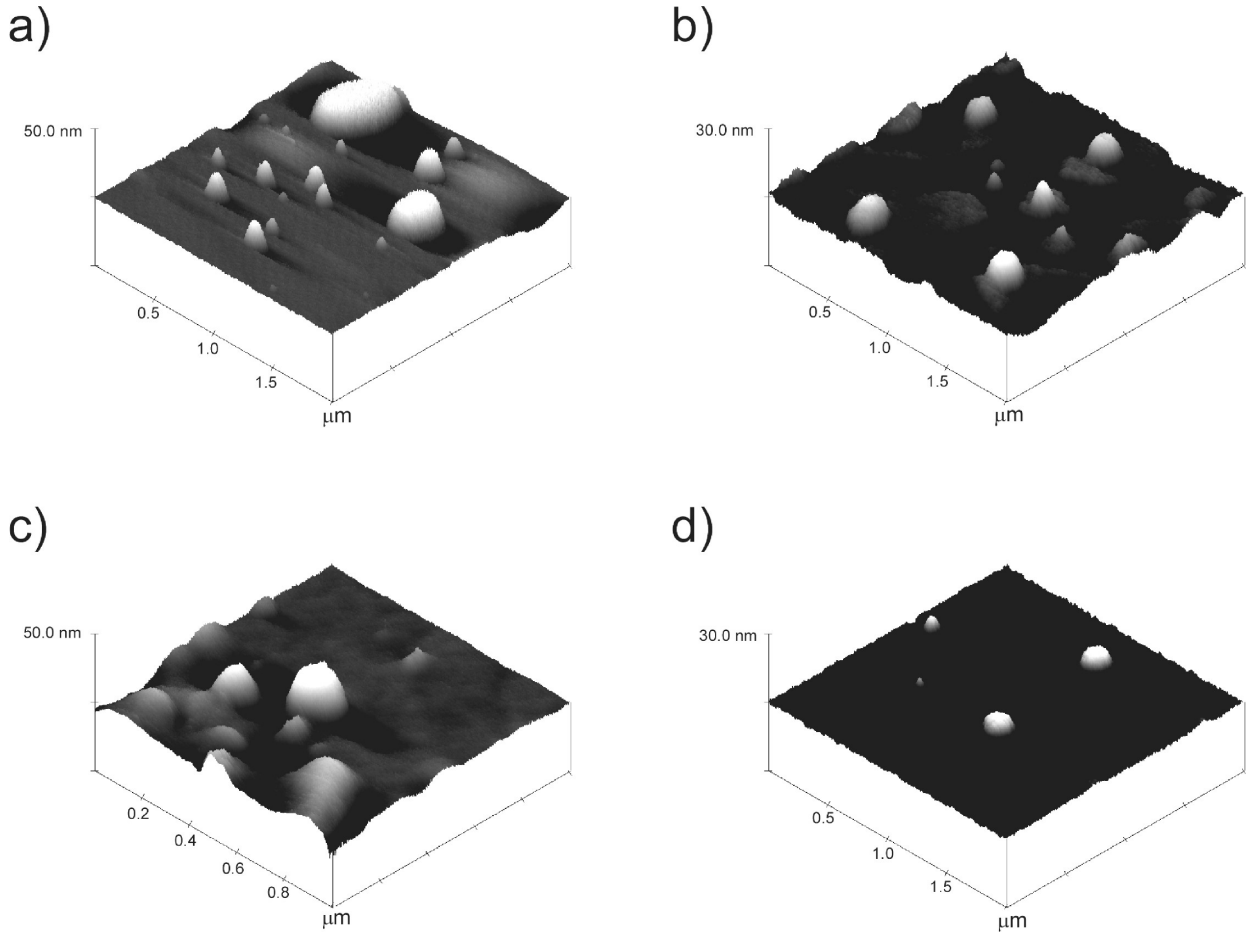

Figure 8. AFM images of PEO-*b*-PIp diblock copolymer inverse assemblies **12**, **13**, **14**, and **15**.

were obtained. In this study, two RAFT-capable PEO macro-CTAs, having M_n values of 2 and 5 kDa, were prepared and used for the polymerization of isoprene, affording block copolymers of varied lengths and compositions. GPC analysis of the PEO macro-CTAs and block copolymers showed remaining unreacted PEO macro-CTA. Following analysis of the GPC chromatograms using mathematical deconvolution, the blocking efficiency was estimated to be around 50% for the 5 kDa PEO macro-CTA and 64% for the 2 kDa CTA. The resultant polymers were also investigated for their abilities to self-assemble in both water and decane, and the resulting regular and inverse assemblies, respectively, were analyzed with DLS, AFM, and TEM to ascertain their dimensions and properties. Assembly of PEO-*b*-PIp block copolymers in aqueous solution resulted in uniform micelles of varying sizes while the assembly in hydrophobic, organic solvent resulted in the formation of heterogeneous morphologies, including large aggregates, cylindrical and spherical structures.

Acknowledgment. This material is based on work supported by the Office of Naval Research under Grant No. N00014-08-1-0398, the National Science Foundation Grant Nos. DMR-0451490 and DMR-0906815, and the National Heart Lung and Blood Institute of the National Institutes of Health as a Program of Excellence in Nanotechnology Grant No. HL080729. The Welch Foundation is gratefully acknowledged for support through the W. T. Doherty-Welch Chair in Chemistry, Grant No. A-0001.

Supporting Information Available: Figures showing thermogravimetric analysis and differential scanning calorimetry results for all polymers, ^{13}C NMR spectra of both CTAs, all available typical DLS plots for micelles, and TEM images of aqueous micelles with OsO_4 staining. This material is available free of charge via the Internet at http://pubs.acs.org.

References and Notes

(1) Blanazs, A.; Armes, S. P.; Ryan, A. J. *Macromol. Rapid Commun.* **2009**, *30* (4−5), 267–277.
(2) Hamley, I. W. *Nanotechnology* **2003**, *14* (10), R39–R54.
(3) Letchford, K.; Burt, H. *Eur. J. Pharm. Biopharm.* **2007**, *65* (3), 259–269.
(4) Pochan, D. J.; Chen, Z. Y.; Cui, H. G.; Hales, K.; Qi, K.; Wooley, K. L. *Science* **2004**, *306* (5693), 94–97.
(5) Li, Z. B.; Kesselman, E.; Talmon, Y.; Hillmyer, M. A.; Lodge, T. P. *Science* **2004**, *306* (5693), 98–101.
(6) Jain, S.; Bates, F. S. *Science* **2003**, *300*, 460–464.
(7) Discher, D. E.; Eisenberg, A. *Science* **2002**, *297* (5583), 967–973.
(8) Zhao, F.; Xie, D. H.; Zhang, G. Z.; Pispas, S. *J. Phys. Chem. B* **2008**, *112*, 6358–6362.
(9) Sundararaman, A.; Stephan, T.; Grubbs, R. B. *J. Am. Chem. Soc.* **2008**, *130*, 12264–12265.
(10) Allen, C.; Maysinger, D.; Eisenberg, A. *Colloids Surf. B: Biointerfaces* **1999**, *16* (1−4), 3–27.
(11) O'Reilly, R. K.; Joralemon, M. J.; Hawker, C. J.; Wooley, K. L. *J. Polym. Sci., Part A: Polym. Chem.* **2006**, *44*, 5203–5217.
(12) Bütün, V.; Billingham, N. C.; Armes, S. P. *J. Am. Chem. Soc.* **1998**, *120*, 12135–12136.
(13) Iijima, M.; Nagasaki, Y.; Okada, T.; Kato, M.; Kataoka, K. *Macromolecules* **1999**, *32* (), 1140–1146.
(14) Simone, E. A.; Dziubla, T. D.; Muzykantov, V. R. *Expert Opin. Drug Deliv.* **2008**, *5*, 1283–1300.
(15) Branco, M. C.; Schneider, J. P. *Acta Biomater.* **2009**, *5*, 817–831.
(16) Kim, B. S.; Park, S. W.; Hammond, P. T. *ACS Nano* **2008**, *2*, 386–392.
(17) Krishnan, R. S.; Mackay, M. E.; Duxbury, P. M.; Pastor, A.; Hawker, C. J.; Van Horn, B.; Asokan, S.; Wong, M. S. *Nano Lett.* **2007**, *7*, 484–489.
(18) Lazzari, M.; Lopez-Quintela, M. A. *Adv. Mater.* **2003**, *15*, 1583–1594.
(19) Mitragotri, S.; Lahann, J. *Nat. Mater.* **2009**, *8* (1), 15–23.
(20) Förster, S.; Antonietti, M. *Adv. Mater.* **1998**, *10*, 195–217.
(21) Soo, P. L.; Eisenberg, A. *J. Polym. Sci., Part B: Polym. Phys.* **2004**, *42*, 923–938.
(22) Zhang, L. F.; Eisenberg, A. *J. Am. Chem. Soc.* **1996**, *118*, 3168–3181.
(23) Gan, Z. H.; Jim, T. F.; Li, M.; Yuer, Z.; Wang, S. G.; Wu, C. *Macromolecules* **1999**, *32*, 590–594.
(24) Shuai, X. T.; Merdan, T.; Schaper, A. K.; Xi, F.; Kissel, T. *Bioconjugate Chem.* **2004**, *15*, 441–448.
(25) dos Santos, A. M.; Le Bris, T.; Graillat, C.; D'Agosto, F.; Lansalot, M. *Macromolecules* **2009**, *42*, 946–956.
(26) Jia, Z. F.; Xu, X. W.; Fu, Q.; Huang, J. L. *J. Polym. Sci., Part A: Polym. Chem.* **2006**, *44*, 6071–6082.
(27) Sun, G.; Hagooly, A.; Xu, J.; Nystrom, A. M.; Li, Z. C.; Rossin, R.; Moore, D. A.; Wooley, K. L.; Welch, M. J. *Biomacromolecules* **2008**, *9*, 1997–2006.
(28) Geng, Y.; Dalhaimer, P.; Cai, S. S.; Tsai, R.; Tewari, M.; Minko, T.; Discher, D. E. *Nature Nanotechnol.* **2007**, *2* (4), 249–255.
(29) Sun, G.; Fang, H. F.; Cheng, C.; Lu, P.; Zhang, K.; Walker, A. V.; Taylor, J. S. A.; Wooley, K. L. *ACS Nano* **2009**, *3*, 673–681.
(30) Rosler, A.; Vandermeulen, G. W. M.; Klok, H. A. *Adv. Drug Delivery Rev.* **2001**, *53* (1), 95–108.
(31) Kohut, A.; Voronov, A.; Samaryk, V.; Peukert, W. *Macromol. Rapid Commun.* **2007**, *28*, 1410–1414.
(32) McCormick, C. L.; Sumerlin, B. S.; Lokitz, B. S.; Stempka, J. E. *Soft Matter* **2008**, *4*, 1760–1773.
(33) Matyjaszewski, K.; Xia, J. H. *Chem. Rev.* **2001**, *101*, 2921–2990.
(34) Moad, G.; Rizzardo, E.; Thang, S. H. *Aust. J. Chem.* **2005**, *58*, 379–410.
(35) Kamigaito, M.; Ando, T.; Sawamoto, M. *Chem. Rev.* **2001**, *101*, 3689–3745.
(36) Hawker, C. J.; Bosman, A. W.; Harth, E. *Chem. Rev.* **2001**, *101*, 3661–3688.
(37) Evans, A. C.; Skey, J.; Wright, M.; Qu, W. J.; Ondeck, C.; Longbottom, D. A.; O'Reilly, R. K. *J. Polym. Sci., Part A: Polym. Chem.* **2009**, *47*, 6814–6826.
(38) Schumers, J. M.; Fustin, C. A.; Can, A.; Hoogenboom, R.; Schubert, U. S.; Gohy, J. F. *J. Polym. Sci., Part A: Polym. Chem.* **2009**, *47*, 6504–6513.
(39) Zhu, J. T.; Hayward, R. C. *J. Am. Chem. Soc.* **2008**, *130*, 7496–7502.
(40) Won, Y. Y.; Davis, H. T.; Bates, F. S. *Science* **1999**, *283* (5404), 960–963.
(41) Mihut, A. M.; Chiche, A.; Drechsler, M.; Schmalz, H.; Di Cola, E.; Krausch, G.; Ballauff, M. *Soft Matter* **2009**, *5* (1), 208–213.
(42) Mueller, W.; Koynov, K.; Fischer, K.; Hartmann, S.; Pierrat, S.; Basche, T.; Maskos, M. *Macromolecules* **2009**, *42*, 357–361.
(43) Allgaier, J.; Poppe, A.; Willner, L.; Richter, D. *Macromolecules* **1997**, *30*, 1582–1586.
(44) Wegrzyn, J. K.; Stephan, T.; Lau, R.; Grubbs, R. B. *J. Polym. Sci., Part A: Polym. Chem.* **2005**, *43*, 2977–2984.
(45) Glynos, E.; Pispas, S.; Koutsos, V. *Macromolecules* **2008**, *41*, 4313–4320.
(46) Gournis, D.; Floudas, G. *Chem. Mater.* **2004**, *16*, 1686–1692.
(47) Förster, S.; Kramer, E. *Macromolecules* **1999**, *32*, 2783–2785.
(48) Benoit, D.; Harth, E.; Fox, P.; Waymouth, R. M.; Hawker, C. J. *Macromolecules* **2000**, *33*, 363–370.
(49) Ruehl, J.; Nilsen, A.; Born, S.; Thoniyot, P.; Xu, L. P.; Chen, S. W.; Braslau, R. *Polymer* **2007**, *48*, 2564–2571.
(50) Pispas, S.; Sarantopoulou, E. *Langmuir* **2007**, *23*, 7484–7490.
(51) Messe, L.; Corvazier, L.; Young, R. N.; Ryan, A. J. *Langmuir* **2002**, *18*, 2564–2570.
(52) Alidedeoglu, A. H.; York, A. W.; McCormick, C. L.; Morgan, S. E. *J. Polym. Sci., Part A: Polym. Chem.* **2009**, *47*, 5405–5415.
(53) Bousquet, A.; Barner-Kowollik, C.; Stenzel, M. H. *J. Polym. Sci., Part A: Polym. Chem.* **2010**, *48*, 1773–1781.
(54) Boyer, C.; Granville, A.; Davis, T. P.; Bulmus, V. *J. Polym. Sci., Part A: Polym. Chem.* **2009**, *47*, 3773–3794.
(55) Gibson, M. I.; Froehlich, E.; Klok, H. A. *J. Polym. Sci., Part A: Polym. Chem.* **2009**, *47*, 4332–4345.
(56) Kakwere, H.; Perrier, S. *J. Polym. Sci., Part A: Polym. Chem.* **2009**, *47*, 6396–6408.
(57) Luzon, M.; Boyer, C.; Peinado, C.; Corrales, T.; Whittaker, M.; Tao, L.; Davis, T. P. *J. Polym. Sci., Part A: Polym. Chem.* **2010**, *48*, 2783–2792.
(58) O'Donnell, J. M.; Kaler, E. W. *J. Polym. Sci., Part A: Polym. Chem.* **2010**, *48*, 604–613.
(59) Vo, C.-D.; Rosselgong, J.; Armes, S. P.; Tirelli, N. *J. Polym. Sci., Part A: Polym. Chem.* **2010**, *48*, 2032–2043.
(60) Germack, D. S.; Harrisson, S.; Brown, G. O.; Wooley, K. L. *J. Polym. Sci., Part A: Polym. Chem.* **2006**, *44*, 5218–5228.

(61) Germack, D. S.; Wooley, K. L. *J. Polym. Sci., Part A: Polym. Chem.* **2007**, *45*, 4100–4108.
(62) Jitchum, V.; Perrier, S. *Macromolecules* **2007**, *40*, 1408–1412.
(63) Germack, D. S.; Wooley, K. L. *Macromol. Chem. Phys.* **2007**, *208*, 2481–2491.
(64) Cauet, S. I.; Wooley, K. L. *J. Polym. Sci., Part A: Polym. Chem.* **2010**, *48*, 2517–2524.
(65) Li, Z.; Zhang, K.; Ma, J.; Cheng, C.; Wooley, K. L. *J. Polym. Sci., Part A: Polym. Chem.* **2009**, *47*, 5557–5563.
(66) Achilleos, M.; Legge, T. M.; Perrier, S.; Patrickios, C. S. *J. Polym. Sci., Part A: Polym. Chem.* **2008**, *46*, 7556–7565.
(67) Li, Y. T.; Lokitz, B. S.; McCormick, C. L. *Macromolecules* **2006**, *39*, 81–89.
(68) Peng, Z. P.; Wang, D.; Liu, X. X.; Tong, Z. *J. Polym. Sci., Part A: Polym. Chem.* **2007**, *45*, 3698–3706.
(69) Walther, A.; Millard, P. E.; Goldmann, A. S.; Lovestead, T. M.; Schacher, F.; Barner-Kowollik, C.; Muller, A. H. E. *Macromolecules* **2008**, *41*, 8608–8619.
(70) Yan, J. J.; Ji, W. X.; Chen, E. Q.; Li, Z. C.; Liang, D. H. *Macromolecules* **2008**, *41*, 4908–4913.
(71) Yusa, S.; Yokoyama, Y.; Morishima, Y. *Macromolecules* **2009**, *42*, 376–383.
(72) Skrabania, K.; Laschewsky, A.; von Berlepsch, H.; Boettcher, C. *Langmuir* **2009**, *25*, 7594–7601.
(73) Xu, X. W.; Smith, A. E.; Kirkland, S. E.; McCormick, C. L. *Macromolecules* **2008**, *41*, 8429–8435.
(74) Jia, Z. F.; Liu, C.; Huang, J. L. *Polymer* **2006**, *47*, 7615–7620.
(75) Lai, J. T. U.S. Patent 6,596,899, 2000.
(76) Kale, T. S.; Klaikherd, A.; Popere, B.; Thayumanavan, S. *Langmuir* **2009**, *25*, 9660–9670.
(77) Gao, H. F.; Tsarevsky, N. V.; Matyjaszewski, K. *Macromolecules* **2005**, *38*, 5995–6004.
(78) *Handbook of size exclusion chromatography and related techniques*, 2nd ed.; Marcel Decker, Inc.: New York, 2004.
(79) Zhang, L. F.; Eisenberg, A. *J. Polym. Sci., Part B: Polym. Phys.* **1999**, *37*, 1469–1484.